

## THE STRAIN ENERGY DENSITY FAILURE CRITERION APPLIED TO NOTCHED ELASTIC SOLIDS

M. E. KIPP and G. C. SIH

Institute of Fracture and Solid Mechanics, Lehigh University,  
Bethlehem, Pennsylvania 18015, U.S.A.

(Received 20 September 1973; revised 18 April 1974)

**Abstract**—Application of the strain energy density failure criterion is made to plane notch problems, where the crack now becomes a special case of a more generalized approach to failure. The specific case considered is that of the plane elliptical cavity under remote tension and compression. Both failure loads and fracture trajectories are discussed. It is shown that an additional characteristic dimension provides satisfactory agreement of the theory with available data. Finally, known characteristics of fracture trajectories from a notch tip are shown to be predicted for unstable fracture conditions.

### 1. INTRODUCTION

The energy density fracture criterion proposed by Sih[1] to predict the failure of elastic solids with cracks is extended to include blunted notches. Since the line crack solution can be recovered as a special case of the blunt notch solution, no special consideration in the prediction of failure is required. Hence, the concept of fracture toughness can be applied to materials containing cracks as well as notches.

Failure criteria applied at the surface of a notch have not been able to explain the failure of notches satisfactorily. This resulted in the development of theories incorporating additional parameters in order to obtain a better description of the geometry effects. Noteworthy are the formulas derived by Neuber[2].

The difficulty was observed by Griffith[3, 4] to be caused by the presence of microcracks, or flaws, at the surface (of silica glass) resulting in a non-continuum surface.

The weakness of brittle materials can be generally attributed to the non-uniform distribution of internal and/or surface flaws. These flaws are inherent in many engineering materials and they also must persist around the edge of a blunt notch. Hence, a failure criterion such as the maximum surface tangential stress may not be able to predict the loads that may be safely applied. Although any theory that attempts to include the surface irregularities would be overwhelmingly complicated, the importance of the surface effect cannot be underestimated. One of the basic assumptions in applying the strain energy density criterion is that the interior must be loaded very nearly to failure in order for a surface initiated fracture to become unstable and propagate through the material. Moreover, while these surface flaws may locally invalidate the continuum solution, the solution remains satisfactory in the bulk of the material.

With these underlying premises, the criterion of strain energy density will be applied to the bulk of the material near the notch surface. Basically, the criterion states that particular stationary values of the strain energy density, as seen from the crack tip dictate the direction and magnitude of the load required for crack extension. As originally proposed by Sih[1], the theory employed the first term expansion of the stresses and strains near the (line) crack tip. Here, the theory is extended to employ the total strain energy density near the notch tip, and the point of reference is chosen to be the location on the surface of the notch where the maximum tangential

stress occurs, since it is expected that from this point, fracture will proceed, although, as stated earlier, failure loads based on this stress are not satisfactory.

Although the symmetric loading cases have received primary consideration, it is now recognized that a knowledge of mixed mode loading is necessary. Earlier data of Erdogan and Sih[5], Cotterell[6] and Williams and Ewing[7] is intended to extend this understanding.

The present considerations are meant to add some theoretical substance to the mixed mode problems. Although in design the symmetric case is usually the weakest case, there do occur non-symmetric configurations where knowledge of the crack path is important.

## 2. LOCAL BEHAVIOR OF THE STRAIN ENERGY DENSITY FUNCTION

The location on the (free) surface of high tension, or tensile stress, may be postulated to be the region of initial failure of the notch. Subsequent behavior, such as the immediate post-failure crack direction, may in part be described by the local features of the strain energy density function. A radius vector,  $r$ , (Fig. 1) is attached to the point of initial surface failure: the vector is of length  $r$ , and its position relative to a fixed axis is given by the angle  $\theta$ , measured positive counterclockwise. The origin of the vector is a function of both loading and notch geometry. Further, for each notch and loading geometry, there is usually a separate origin for the tension and compression cases.

In order to utilize the strain energy density function as a failure criterion, it is necessary to have at least a qualitative view of the nature of its behavior around a notch tip. Presuming temporarily that the structure containing the notch is only slightly loaded and that the material near the notch is perfectly elastic, contours of constant strain energy density generated by the presence of the notch would qualitatively appear as shown in Fig. 2: the inner contours are those of higher density, and the outer ones of lower density. The contours are emanating roughly from the location of the maximum surface tangential stress. Attached to this location is the radius vector  $r$ . Figure 2 also indicates that were  $r$  fixed, and  $\theta$  permitted to vary, the resulting circular

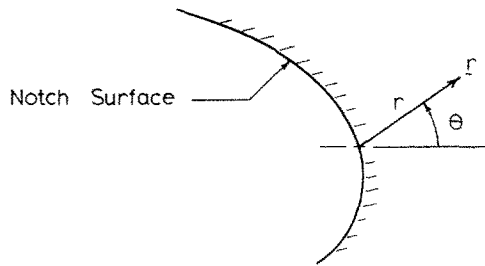


Fig. 1. Components of the radius vect  $r$ .

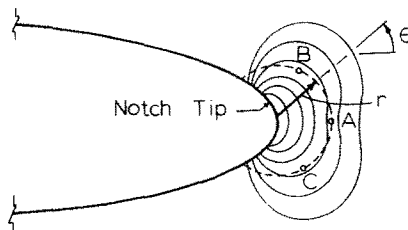


Fig. 2. Radius vector locus intersecting strain energy density contours.

locus intersects varying strength contours of strain energy density, and, it is expected that for a given magnitude of the radius, several stationary values of the strain energy will be acquired at discrete values of the angular parameter. In terms of the angle  $\theta$ , the variation in strain energy density encountered by the constant magnitude radius vector is illustrated by the curve in Fig. 3. It is observed that, in general, more than one stationary value is observed: a minimum at  $A$ , maxima at  $B$  and  $C$ ; the actual number depends upon the material and geometry involved. In accordance with the theory as advanced by Sih [1], the minimum at  $A$  may be associated with the load for failure, which is determined from the critical material value of the strain energy density, and is dependent upon the specific radius chosen. Specific choice of the appropriate value of  $r$ ,  $r_0$ , requires experimental data for a given material: it is expected that  $r_0$  so chosen will be a constant for the material, and hence, knowledge of failure loads for one geometry may easily be used to determine failure loads for other geometries.

In addition to determining failure loads, it does not seem unreasonable to assert that the initial notch and loading geometries (and material properties) may determine not only the load required to precipitate fracture and the initial fracture angle, but also the subsequent path the fracture will follow. That is, upon being loaded, the notch must seek a path of release, through knowledge of the local properties of the strained material, seen from its *present configuration*. Once loading is initiated, it should be immediately clear from the geometry on exactly what path the fracture will proceed, leaving as the only undetermined factor that of fulfilling the actual initiation of the fracture. There are, however, many configurations for which crack growth is [globally] stable; one in particular involves the loading of a punch resting on a glass block [8]. As the load is increased, the crack grows a corresponding amount, stops, and remains stationary until a further load increase occurs. Under such conditions, long range path predictions would not be possible. In the configurations where local and global instability occur simultaneously, such as notches loaded uniformly at distances far from the notch, crack growth is quite sudden and unstable<sup>†</sup>. Then the material has no time to readjust to a new configuration, and as suggested above, quite possibly, at least the initial fracture path is predetermined. The argument in favor of such behavior comes from an understanding of the global energy field: in brittle materials, for blunt notches, or line cracks at low angles of loading, the loads required for initial fracture are relatively high (when compared to that of the line crack in symmetric loading) so that there already exists a high density energy in the regions at both near and far distances from the point of incipient failure. Such a field will do much to contribute to rapid fracture and failure, when few available physical resources exist to inhibit the fracture from propagating.

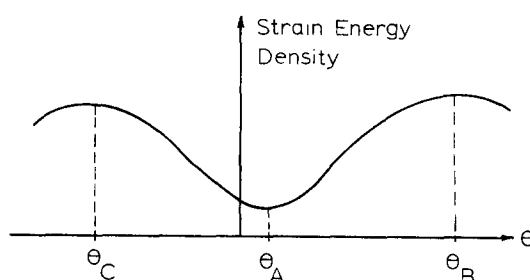


Fig. 3. Variation of strain energy density, for constant magnitude radius vector, as function of angular parameter.

<sup>†</sup>This is consistent with the physical phenomenon of buckling: if the buckling is unstable, then the post-buckling behavior is predetermined.

In order to determine a path for the fracture, the family of curves generated for a wide range of radius vectors provides the locations of the sequence of points that indicated stationary values of the strain energy function. It is here suggested that this trajectory should be in close agreement with the actual fracture path taken from a notch on a brittle material. Under these circumstances, it is evident that the maximum tangential stress requires a reference point for the angular variation *that follows the path of fracture*, whereas the strain energy methods described may observe the whole field from one vantage point—that at the notch surface. This is a consequence of the local orientation invariance of the strain energy density. Subsequent discussion of a specific example will bear out the expected accuracy of the path prediction capabilities.

In plane problems, the general form of the strain energy density function is given by

$$\frac{dW}{dA} = \frac{1}{16\mu} [(1 + \kappa)(\sigma_{11}^2 + \sigma_{22}^2) - 2(3 - \kappa)\sigma_{11}\sigma_{22} + 8\sigma_{12}^2] \quad (1)$$

where  $\kappa$  is defined to be  $3 - 4\nu$  for plane strain and  $(3 - \nu)/(1 + \nu)$  for plane stress, and  $\mu$  is the shear modulus. The approach of Sih[1] has been to substitute the first term of the asymptotic expansions for the stresses into (1) to obtain

$$\frac{dW}{dA} = \frac{S}{r} \quad (2)$$

where  $S$  is a function of the stress intensity factors and the angular parameter  $\theta$ . For a fixed distance  $r_0$ , one may then use

$$S = r_0 \left( \frac{dW}{dA} \right) \quad (3)$$

so that  $S$  assumes some critical value,  $S_{cr}$ , which characterizes the toughness of the material.

In the present considerations, the exact stresses are substituted into (1), and the radius,  $r$ , may no longer be factored from the expression. However, from (3), it is seen that specifying  $S_{cr}$  to be a constant is equivalent to requiring that  $(dW/dA)_{cr}$  be a constant; then numerical procedures may be employed to determine critical loads once the value of  $r_0$  has been chosen, and the stresses for a given geometry are substituted into (1). Since  $r$  specifically may not be zero, geometric singularities will no longer require special consideration.

It should be noted that some of the results subsequently described differ little with those found by the maximum tangential stress theory; the strain energy density theory is expected to hold not only for these conditions, but a much wider range of physical situations as well, i.e. not discrediting the former, but providing a more consistent framework for the prediction of material failure [16].

### 3. THE PLANE ELLIPTICAL CAVITY—FAILURE LOADS

The elliptical cavity (in two dimensions—plane strain) is defined by the ratio of minor to major axis half-lengths,  $b/a$ , with all other length parameters normalized with respect to the major axis half-length,  $a$ . The uniform loading (at infinity) forms an angle of  $\beta$  with the major axis of the cavity, and the angle  $\theta$  used in the radius vector  $r$  is measured positive counterclockwise, referenced to an axis parallel to the major axis of the cavity. At any given point on the surface of the cavity, the normal angle to the surface forms an angle  $\phi$  with the major axis, and also is measured positive counterclockwise. Figure 4 indicates the geometry described. Only the right

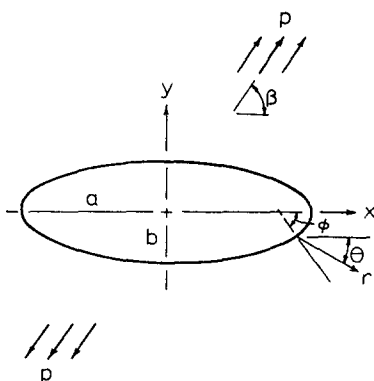


Fig. 4. Geometry and parameters of elliptical cavity and radius vector.

hand notch tip will be considered, as antisymmetry of the geometry implicitly allows description of the other notch tip as well.

The stresses for this geometry are well known, and in this case, those given by Muskhelishvili[9] were used. The strain energy density function for the cavity is obtained by substitution of the given stresses into equation (1). Both this and the acquisition of stationary values were performed numerically. Poisson’s ratio was arbitrarily chosen to be 0.25, except where noted for specific data comparison. It is clear from the work of Sih[1] that there are significant variations attributable to Poisson’s ratio change, and this will not be further illustrated.

The origin of the radius vector *r* is taken at the location along the boundary of the maximum tangential tensile stress. For the elliptical cavity, this position may be analytically determined to be

$$\tan \eta = \frac{b[a \sin^2 \beta - b \cos^2 \beta \pm \sqrt{a^2 \sin^2 \beta + b^2 \cos^2 \beta}]}{a(a + b) \sin \beta \cos \beta} \tag{4}$$

Two values of the eccentric angle  $\eta$  are obtained: the positive root provides the origin for compressive loading, and the negative root for tensile loading, (Fig. 5).

(a) *The case of tension*

As noted, the eccentric angle  $\eta$  that locates the origin of *r* is the negative root given by (4). Figures 6–8 indicate the variation in stationary values (minima) acquired for specific values of

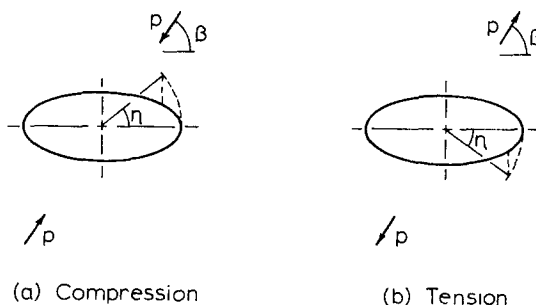


Fig. 5. Location of points of initial failure in tension and compression.

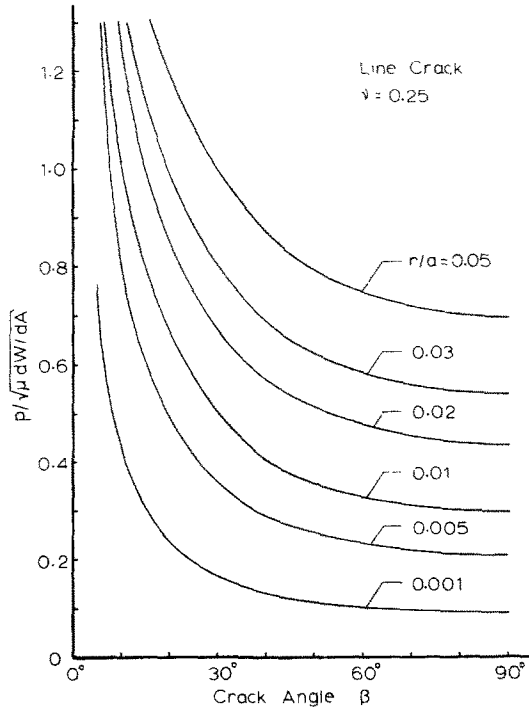


Fig. 6. Variation of load with crack angle: line crack; (tension).

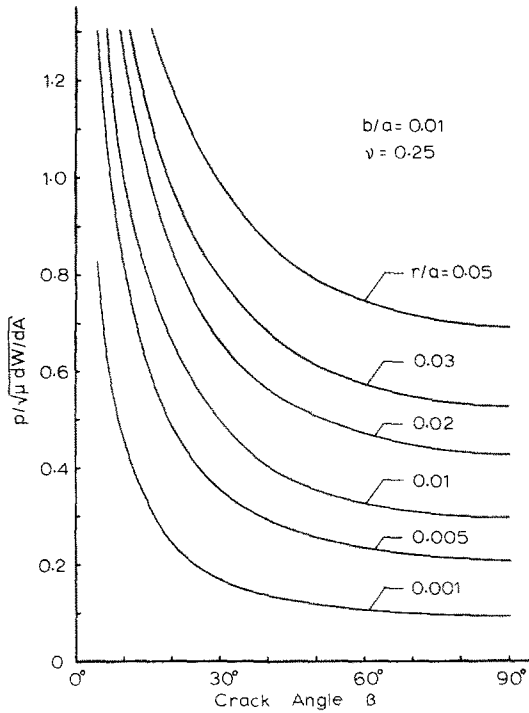


Fig. 7. Variation of load with crack angle:  $b/a = 0.01$ ; (tension).

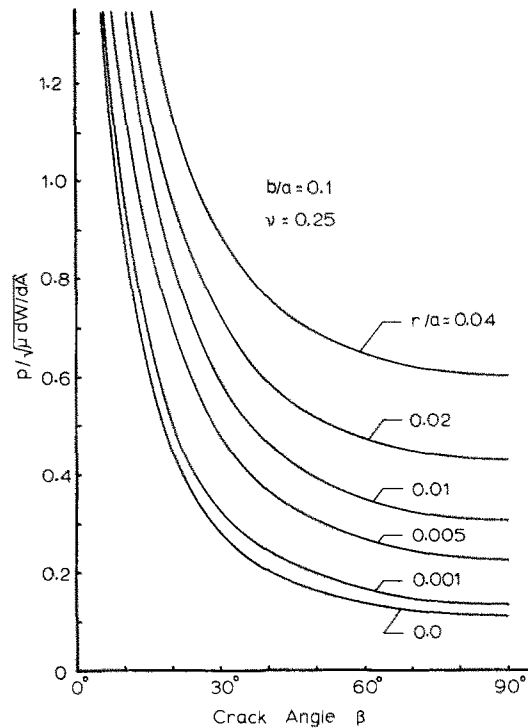


Fig. 8. Variation of load with crack angle:  $b/a = 0.1$ ; (tension).

$b/a$ , loading angle  $\beta$ , and radius  $r$ . For any particular combination of values, the angle  $\theta$  is varied until the minimum is determined; at this value of  $\theta$ , the corresponding load is obtained, and plotted in the following figures. It may be observed that in all cases the minimum load required for fracture occurs in the normal loading case ( $\beta = 90^\circ$ ). Intuitively, one would expect such a result, although other fracture criteria have been proposed in which the minimum load appears in the vicinity of  $\beta = 70^\circ$ . Palaniswamy [10] attempted an energy release rate procedure for complex loading, in which a small extension to the main crack was varied in direction until the maximum strain energy release rate for small crack extension was determined; in this case, a minimum was located near  $72^\circ$ . A second case in which the minimum load appears near  $\beta = 70^\circ$  occurs in the criterion of maximum tangential stress near the crack tip. Unmentioned in the original paper on the inclined loading of a crack by Erdogan and Sih [5], Williams and Ewing [7] pointed out this effect in the loading response. This latter work included an attempt to avoid the local material behavior by applying the criterion a short distance from the crack tip using an additional term in the asymptotic solution. Unfortunately, the truncation errors in the results overemphasize the minimum load, manifest when compared to the exact solution (Sih and Kipp [11]). (In this reference, the strain energy density theory is shown to agree very well with the tensile data of Williams and Ewing [7], and will not be reproduced here). At  $\beta = 0^\circ$ , a material with a line crack behaves as if no flaw were present, but where the crack is blunted, finite loads to failure will occur: these loads occur off-axis in Figs. 7 and 8, and are non zero in general for  $b/a > 0$ .

Figures 6–8 also reflect the trend of the increased loading permitted as the notch tip becomes more blunted. If an elliptical cavity is experimentally loaded to failure at several crack angles, then from the corresponding family of curves for the same size notch, the curve that matches the

data may be extracted, and that choice will provide the characteristic dimension,  $r_0$ , assuming that the elastic strain energy density constant is known. A knowledge of these two parameters has been earlier postulated to be sufficient to describe the failure of this material in the presence of any geometric configuration, whether line crack or notch. In the case at hand, given  $r_0$ , a family of curves may now be established that indicates the change in loading patterns as the geometry changes. For example, should  $r_0/a = 0.01$ , then for various values of  $b/a$ , the variation in loading appears as in Fig. 9. The value of the angled crack problem should now be more clearly seen: the failure criterion is based not on a single load to failure, but a function, and while more difficult to obtain, in principle, the prediction reliability should be considerably greater than presently is the case.

(b) *The case of compression*

Although much of the behavior to be described in this section corresponds to that of the tensile case, there are a few additional difficulties that must be dealt with in compression. Rather than reiterating the arguments already presented in detail, emphasis will be placed upon the features that tend to complicate the compressive analysis. Were the analysis confined to simply reversing the applied loads in the last section and proceeding as before, there would be no trouble. But immediately, caution must be exercised in requiring that no interpenetration of notch faces occurs. The line crack, for instance, must be reformulated to ensure that sufficient normal stresses occur on the faces to prevent penetration, and this has been attempted by McClintock and Walsh [12]. In addition, it is clear that functional stresses will be developed on the faces if any

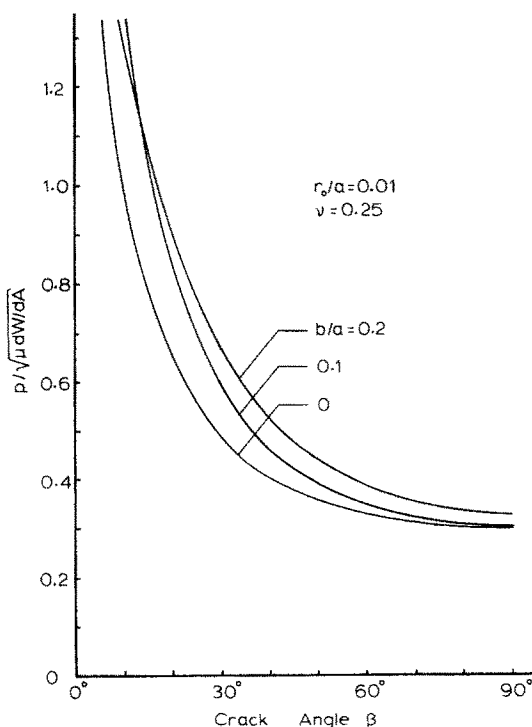


Fig. 9. Variation of load with geometry for fixed core dimension:  $r_0/a = 0.01$ ; (tension).



slip is to occur to allow fracture to progress. In the development here, the notch geometry will be restricted to such dimensions that contact between opposing faces cannot occur.

The geometry of the ellipse is such that in compression, the maximum surface tangential stress that may develop is equal in magnitude to little more than the applied compressive load, and elsewhere, tremendous crushing pressures may be developed. The consequence is that some kind of material damage is inevitable, although it does occur at locations away from where a fracture is expected to initiate and grow. A combination of these factors results in a weaker model for fracture prediction than that of the tension case, although limited agreement with experimental data does occur.

As before, assuming a small applied uniform stress, the surface position of maximum energy (maximum surface tangential stress) may be located, and an origin established to evaluate the load behavior as a function of radial distance from the surface. Figures 10 and 11 describe the load behavior as a function of notch angle, for various constant radii,  $r/a$ .

Once a characteristic dimension has been established, say  $r_0/a = 0.01$ , the variation in load with geometry may be described, as in Fig. 12. For a given material, and the present analysis, it is expected that a value of  $r_0/a$ , must be determined, since in general, the behavior of a material in compression differs considerably from that in tension. That is to say, another sequence of tests would be required to obtain the dimension,  $r_0$ , and in a general analysis, one necessarily would need to know the expected geometry and loading conditions before deciding upon the critical parameters involved in load prediction.

A characteristic of compressive loading is the minimum load to fracture occurrence in the non-symmetric case. The families of curves plotted indicate a wide range of failure loads over the various values of  $\beta$  from zero to normal, but experimentally, there exists much less variation. Cotterell[6] has published the experimental data that appear in Fig. 13 for an elliptical cavity,  $b/a = 0.1$ , in glass. The curves in this figure are those of Fig. 11, normalized to the load at  $\beta = 90^\circ$ . The curve  $r/a = 0$  is that of the maximum tangential stress criterion. As the position of failure

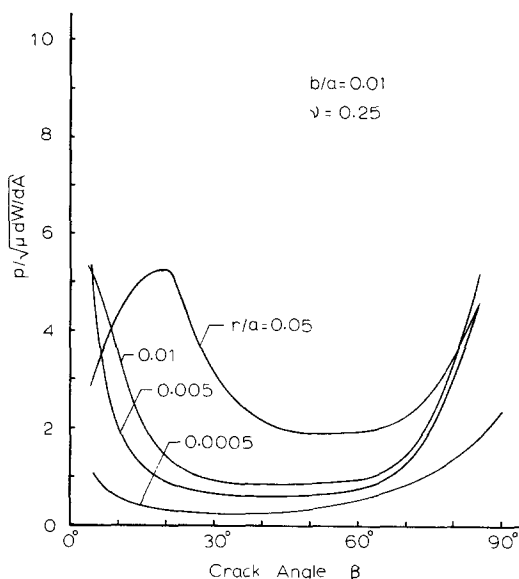


Fig. 10. Variation of load with crack angle:  $b/a = 0.01$ ; (compression).

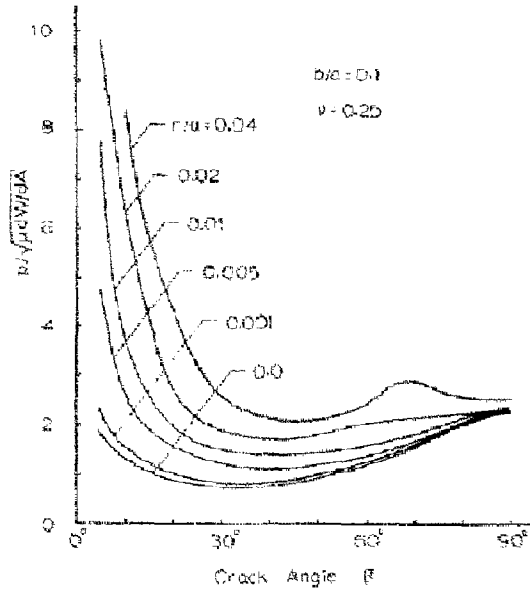


Fig. 11. Variation of load with crack angle:  $b/a = 0.1$ ; (compression).

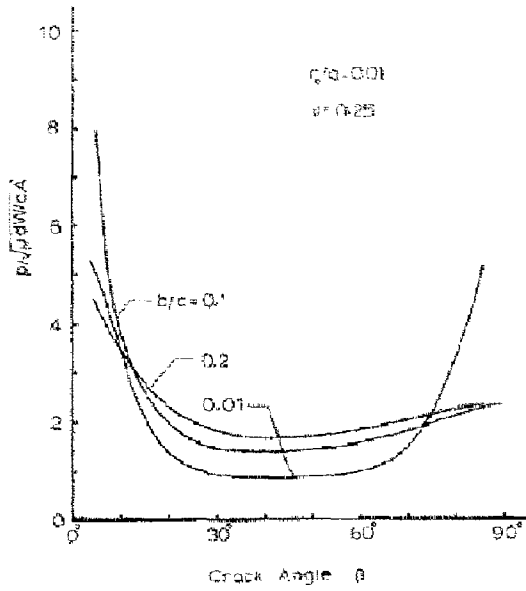


Fig. 12. Variation of load with geometry for fixed core dimension:  $r/a = 0.01$ ; (compression).

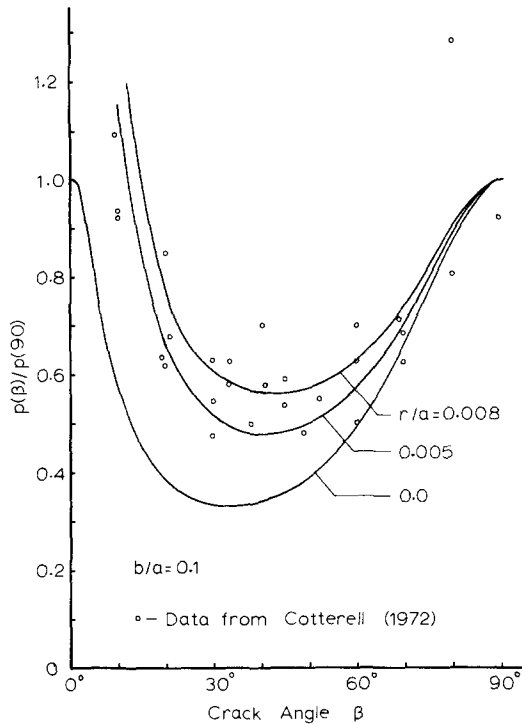


Fig. 13. Variation of load with crack angle:  $b/a = 0.1$ ; data from Cotterell (1972); (compression).

criterion is moved into the material, there appears quite satisfactory agreement between  $r/a = 0.005$  and  $0.008$ . Hence the energy criterion may be expected to provide reasonable failure predictions. On the basis of the data, one could choose a critical dimension of, say,  $r_0/a = 0.005$ , and then use this dimension as set forth in previous sections for load predictions for other geometries in this material.

#### 4. THE PLANE ELLIPTICAL CAVITY—FRACTURE TRAJECTORIES

Although interest from a safety standpoint centers on loading capacity, and more specifically, on the worst case if possible, the actual post-failure behavior of the fracture provides another insight into the validity of the theory under study. As briefly mentioned earlier, Griffith had suggested that a crack would extend in a direction normal to the maximum tangential stress, and Erdogan and Sih [5], in applying this criterion obtained striking agreement with their experimental data. In a discussion of this paper, McClintock [13] suggested the use of the normal angle from the ellipse surface as the directional property, but the result was not in the slightest agreement with the observed behavior. The published data of Williams and Ewing [7] for initial crack angle (with respect to the plane of the crack) corroborates that of Erdogan and Sih. In tension, at  $\beta = 90^\circ$ , the crack is expected to propagate in its own plane, but as  $\beta$  becomes small, the direction becomes less well defined. At  $\beta = 0$ , the material reacts as if (in theory) no crack at all were present, and while the material would be expected to break at a normal to the load, the crack solution cannot predict this. Before proceeding further, it is necessary to be more precise in stating how the crack will extend from the tip of the crack or notch. When the stationary values of the strain energy density were determined for various radius vectors, in addition to the load, an angle  $\theta$  was found

corresponding to the load. So for each radius  $r/a$ , a curve is generated in the angle  $\theta$ ; Figures 14-16 reflect this angle for the same ratios of  $b/a$  and  $r/a$  as used for the load variations of Figs. 6-8. Once the parameter  $r_0/a$  has been established from loading considerations, the angle of fracture,  $\theta_0$ , is determined from the assumption that there is separation of the material from the surface in the direction  $\theta_0$ , with subsequent fracture proceeding from there. If  $r_0/a$  is taken to be 0.01, corresponding to the load example, then for varying ratios of  $b/a$ , the resulting alterations in initial fracture angle would appear as in Fig. 17.

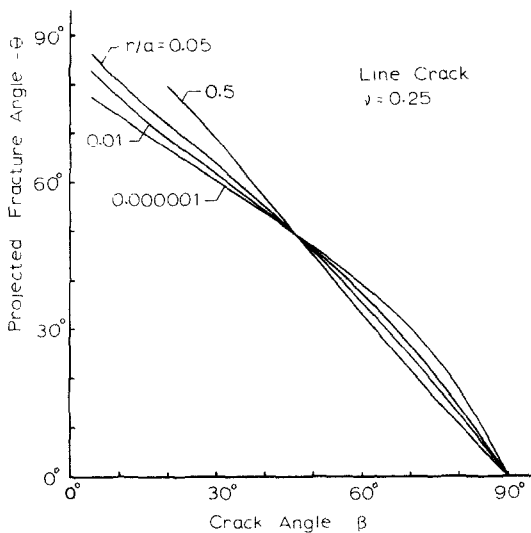


Fig. 14. Variation of fracture angle with crack angle: line crack; (tension).

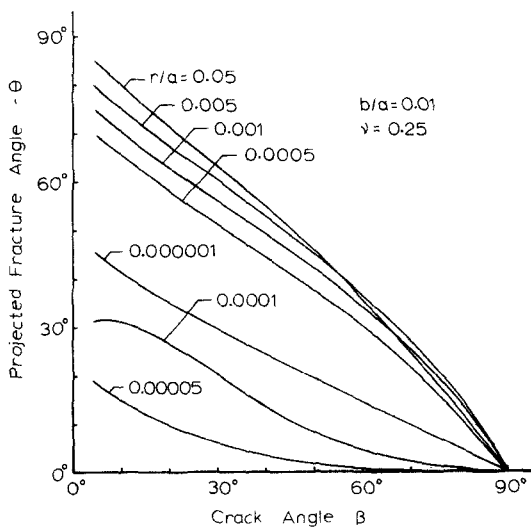


Fig. 15. Variation of fracture angle with crack angle:  $b/a = 0.01$ ; (tension).

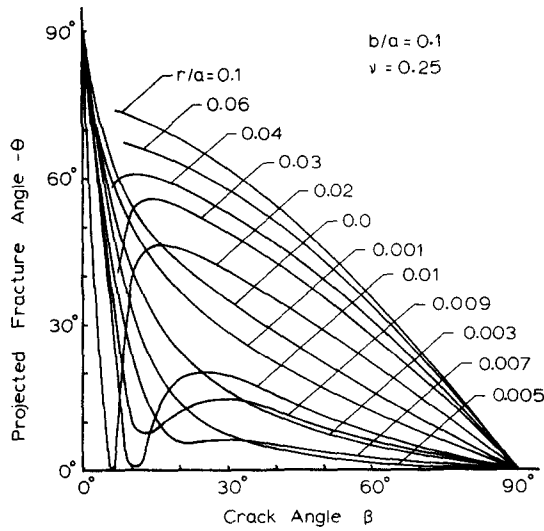


Fig. 16. Variation of fracture angle with crack angle:  $b/a = 0.1$ ; (tension).

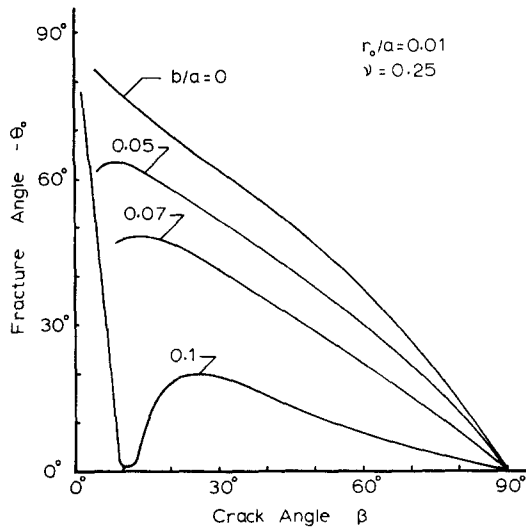


Fig. 17. Variation of fracture angle with crack angle for fixed core dimension:  $r_0/a = 0.01$ ; (tension).

One must remain cognizant of the non-stationary position of fracture initiation along the notch surface. As the loading angle changes, so does the position of initial failure. One result is that now, when  $\beta = 0$ , there is a well defined point of failure (because the geometry is now nontrivial), and it is to be expected that the fracture will extend from the minor edge of the cavity along the minor axis direction. The path is, of course, perpendicular to the load, and the behavior, apart from load magnitude, corresponds exactly to that from the major axis notch tip at  $\beta = 90^\circ$ .

Cotterell [14] has observed that for notches, rather than immediately turning into a path of fracture coinciding with that of the line crack, the fracture trajectory extends forward from the notch tip, roughly in the same plane, for a distance of approximately one notch tip radius, before

turning into the path direction matching that for the line crack. (The ideal line crack has, of course, no tip radius, and would immediately assume its characteristic direction of failure). If it is assumed that the crack path is predetermined for initially brittle materials in unstable configurations, then the radius vector  $r = r(\theta)$  should trace out the trajectory along which fracture is expected to occur. In effect, the trajectory will follow a path that restores symmetry to the geometry of fracture.

For a line crack in tension, Fig. 18 illustrates the projected path for several angles of loading. Photographs† of actual crack trajectories are shown in Figs. 19(a), 19(b), and 19(c), for angles of loading  $\beta = 30^\circ, 45^\circ,$  and  $60^\circ,$  respectively. Attached to each photograph is a trace of the mathematically predicted path, for a crack of the size shown in the photograph. The agreement is observed to be very good for the cases included, out to a distance of at least one-half crack length.

If the behavior of a rather blunt notch, say  $b/a = 0.1,$  is examined, an overall view (Fig. 20) suggests that there have been at least some local changes in behavior from that of the line crack. Upon close observation, the trajectories near the surface reveal a behavior that connects some previously advanced, but analytically unsupported, ideas. When the surface of the notch separates, the fracture begins its course tangentially to the normal angle at the surface; i.e. initial fracture is perpendicular to the surface, coinciding with McClintock's [13] hypothesis. But this is only a local tangent, for the path then bends sharply towards the horizontal (with respect to the major axis of the notch), and extends in this way for a short distance. Again, a sharp turn occurs, now into a direction whose tangent matches that for the initial fracture angle of the line crack.

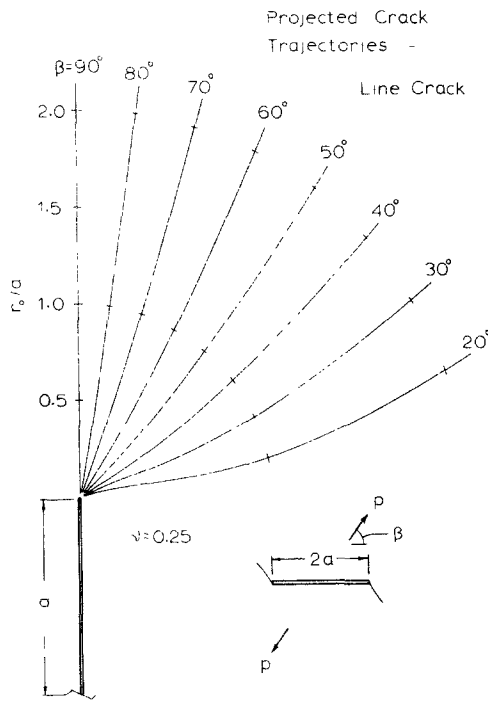


Fig. 18. Projected fracture trajectories: line crack; (tension).

†Appreciation for these photographs is expressed to Dr. T. T. Wang, Bell Telephone Laboratories, Murray Hill, New Jersey.

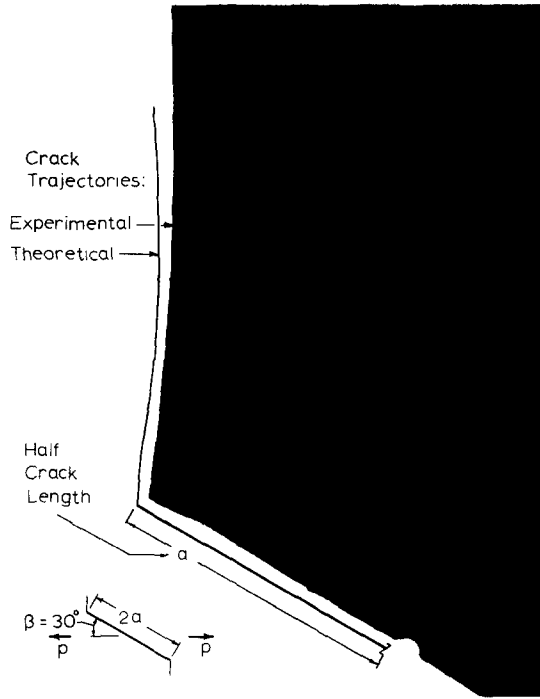


Fig. 19(a). Predicted and experimental fracture trajectories:  $\beta = 30^\circ$ .

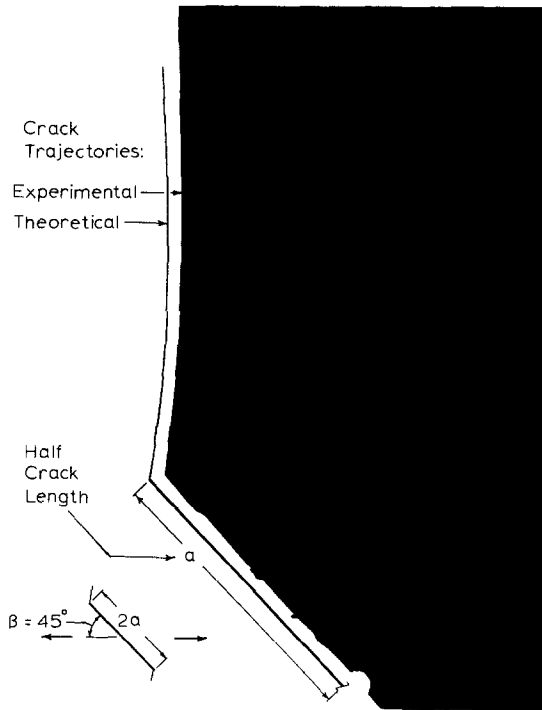


Fig. 19(b). Predicted and experimental fracture trajectories:  $\beta = 45^\circ$ .

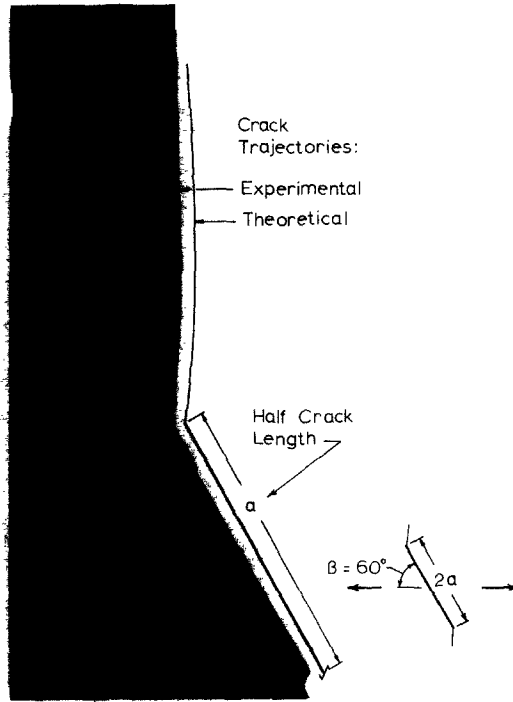


Fig. 19(c). Predicted and experimental fracture trajectories;  $\beta = 60^\circ$ .

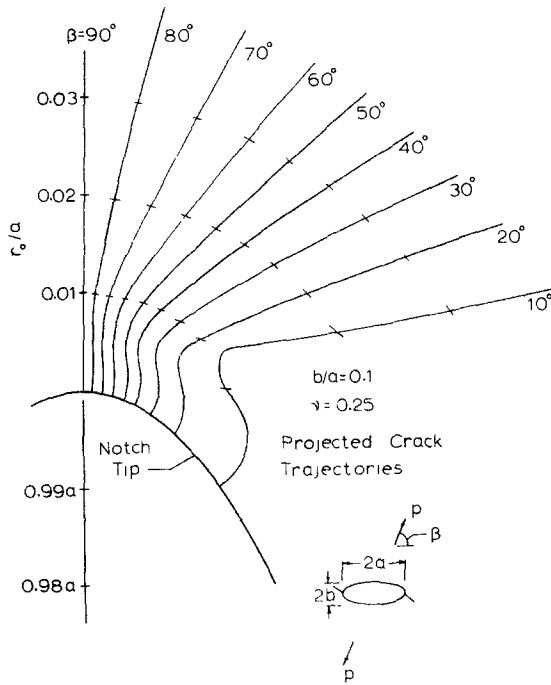


Fig. 20. Projected fracture trajectories:  $b/a = 0.1$ ; (tension).



The short extension distance is approximately equal to the notch tip radius, in accordance with the observations of Cotterell [14]. Subsequent to turning onto the path of fracture coinciding with that of the line crack, the trajectory continues in much the same manner as that of the line crack.

These latter observations have been made assuming prevailing linear elastic response both locally and globally. Should there be extensive localized inhomogeneity, or unaccountable grain size effects, it is expected that few of the above phenomena will be observable, and a more refined model must be created to determine the local behavior. Also, if the fracture is slow, then the material has time to react to the new geometry, and the details listed above are no longer valid.

Under uniform loads, it has been observed that propagating tensile cracks tend to restore symmetry by running normal to tensile loads, and parallel to compressive loads. It is expected that for the elliptical cavity under compression, for loads parallel to the major axis, and extend along that same axis towards the applied load, while for loads parallel to the minor axis, fracture will initiate at the surface intersection with the minor axis, and again extend towards the applied load; i.e. for  $\beta = 0^\circ$ ,  $\theta_0 = 0^\circ$  and for  $\beta = 90^\circ$ ,  $\theta_0 = 90^\circ$ . Between these two limiting cases, the behavior is determined as in the tensile loading case: the stationary values of  $\theta$  are plotted as functions of crack angle  $\beta$ , for various magnitudes of  $r$  (Figs. 21 and 22). It must be emphasized that not until a specific dimension  $r_0$  has been obtained can any of these curves represent the initial fracture angle. If, for example,  $r_0/a = 0.01$ , then the initial fracture angle, as it varies with geometry, is given by Fig. 23. The data shown in Fig. 24 is from Cotterell [6] for elliptical cavities

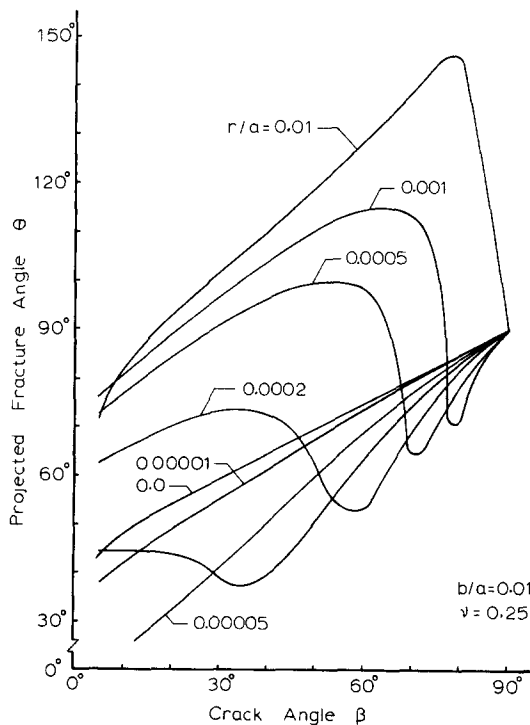


Fig. 21. Variation of fracture angle with crack angle:  $b/a = 0.01$ ; (compression).

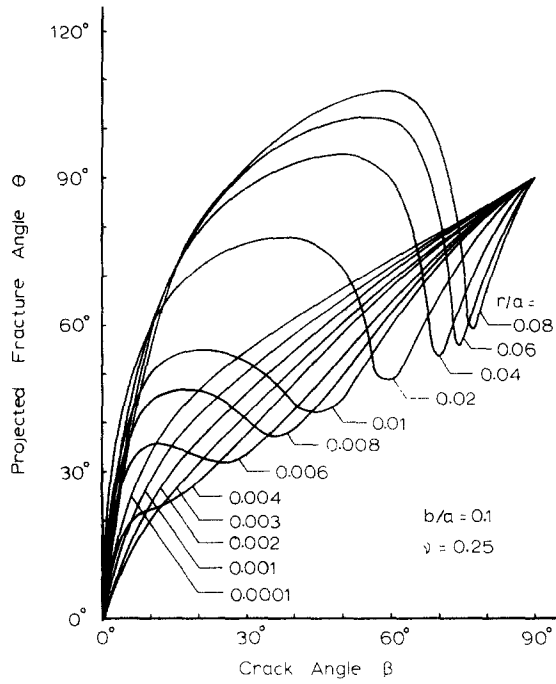


Fig. 22. Variation of fracture angle with crack angle:  $b/a = 0.1$ ; (compression).

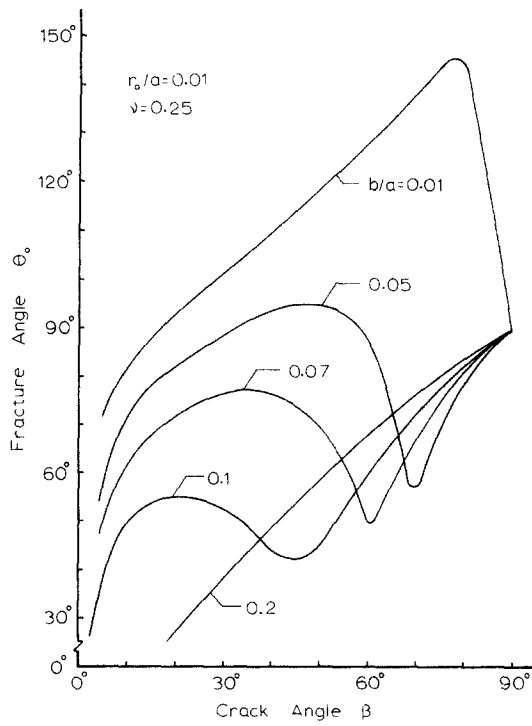


Fig. 23. Variation of fracture angle with crack angle for fixed core dimension:  $r_0/a = 0.01$ ; (compression).

in glass plates loaded in compression. The curves are those from Fig. 22, since the data is for cavities of ratio  $b/a = 0.1$ .

The lower curves presented in Fig. 24 are for small values of  $r/a$ . The upper curve represents the tangent angle taken from the plots in Figs. 25 and 26, of the crack trajectory after it makes the sharp turn into its final path.

In general, the loads required to cause failure in compression are substantially higher than those in tension, and there results throughout the member severely strained material, so that there is a high energy density prevailing<sup>†</sup>. The locus of stationary values,  $r$ , may be plotted to attempt to predict the subsequent path taken by the fracture (Figs. 25 and 26). As in the tension case, the path is initially tangent to the local normal before bending away; then there is a quick return into the general trend leading the path towards the uniform load. This describes the behavior for most of the angles of loading; apparently, as  $\beta$  increases, so does the length of the initial trajectory before its final turn into the load. This is also evident by following changes in  $r/a$  for constant  $\beta$  in Figs. 21 and 22.

In view of the trajectories in both tension and compression, especially the local changes that occur when blunting is present, a vital piece of information to be given with the initial fracture angles is the location of measurement. In part, this is the missing factor in the curves of Fig. 24, since it is really now known where the tangent was taken to obtain the fracture angles. In general, the theory as presented requires this additional length parameter to correlate experimental and theoretical behavior more accurately.

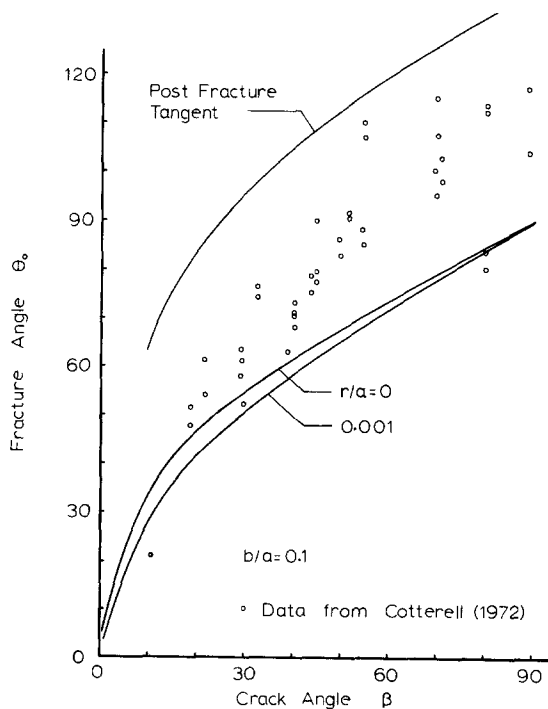


Fig. 24. Variation of fracture angle with crack angle:  $b/a = 0.1$ ; data from Cotterell [6]; (compression).

<sup>†</sup>The results are expected to hold for final catastrophic failure, but not to account for preliminary damage that accrues on the notch surface.

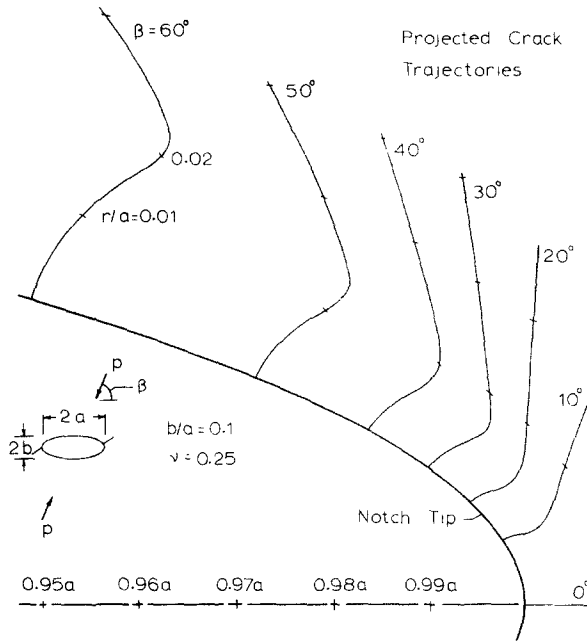


Fig. 25. Projected fracture trajectories:  $b/a = 0.1$ ; small angles of loading; (compression).

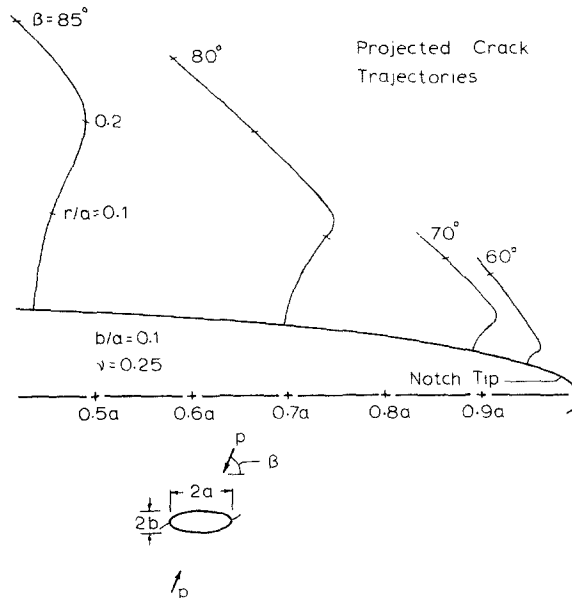


Fig. 26. Projected fracture trajectories:  $b/a = 0.1$ ; large angles of loading; (compression).

## 5. CONCLUDING REMARKS

The aim of this approach to a more unified theory of cracks and notches is to obtain a fracture toughness parameter that may be generally applied; i.e. a true material constant.

It is now evident that at the stationary values of the strain energy density obtained, the division of the strain energy into dilatational and distortional parts provides a deeper understanding of the mechanism of fracture [15]. This suggests the possibility of extending the analyses to ductile materials, where directly in front of the crack tip there is little or no plastic deformation. Hence, the same fracture toughness criterion can be applied to this elastic region once the yielded regions have been obtained.

## REFERENCES

1. G. C. Sih, A Special Theory of Crack Propagation, *Methods of Analysis and Solutions to Crack Problems*, edited by G. C. Sih. Wolters-Noordhoff (1973).
2. H. Neuber, *Theory of Notch Stresses*, Edwards, Michigan (1946).
3. A. A. Griffith, The Phenomena of Rupture and Flow in Solids, *Phil. Trans. Roy. Soc. London*, Ser. A221, 163–198 (1921).
4. A. A. Griffith, The Theory of Rupture, *1st Int. Cong. for Appl. Mech.*, Delft, pp. 55–63 (1924).
5. F. Erdogan and G. C. Sih, On the Crack Extension in Plates Under Plane Loading and Transverse Shear, *J. Basic Eng.*, **85**, 519 (1963).
6. B. Cotterell, Brittle Fracture in Compression, *Int. J. Frac. Mech.* **8**, 195–208 (1972).
7. J. G. Williams and P. D. Ewing, Fracture Under Complex Stress—the Angled Crack Problem, *Int. J. Frac. Mech.* **8**, 441–446 (1972).
8. F. C. Roesler, Brittle Fractures near Equilibrium, *Proc. Phys. Soc.* **B69**, 981–992 (1956).
9. N. I. Muskhelishvili, *Some Basic Problems of the Mathematical Theory of Elasticity*. Noordhoff, Groningen, Holland (1953).
10. K. Palaniswamy, Crack Propagation Under General In-Plane Loading, Ph.D. Dissertation, Cal. Inst. Tech. (1972).
11. G. C. Sih and M. E. Kipp, Discussion on Williams and Ewing (1972), *Int. J. Frac. Mech.* **10**, 261 (1974).
12. F. A. McClintock and J. B. Walsh, Friction on Griffith Cracks in Rocks Under Pressure, *Proc. 4th U.S. Nat. Cong. Appl. Mech.*, pp. 1015–1021 (1962).
13. F. A. McClintock, Discussion of Erdogan and Sih (1963), *J. Basic Eng.*, **85**, 525–527 (1963).
14. B. Cotterell, The Paradox Between the Theories for Tensile and Compressive Fracture, *Int. J. Frac. Mech.*, **5**, 251–252 (1969).
15. G. C. Sih and B. Macdonald, Fracture Mechanics Applied to Engineering Problems—Strain Energy Density Fracture Criteria, *J. Eng. Frac. Mech.*, in press.
16. G. C. Sih, Discussion on 'Some Observations on Sih's Strain Energy Density Approach for Fracture Prediction', authored by I. Finnie and H. O. Weiss, *Int. J. Frac. Mech.*, **10**, 279 (1974).